Available online at www.sciencedirect.com

ScienceDirect

Procedia CIRP 108 (2022) 317–322

www.elsevier.com/locate/procedia

6th CIRP Conference on Surface Integrity

Enhancing surface integrity of A7050-T7451 aluminium alloy by pneumatic machine hammer peening

A. Madariaga[a]*, M. Cuesta[a], E. Dominguez[a], A. Garay[a], G. Ortiz-de-Zarate[a], P.J. Arrazola[a]

a) Mondragon Unibertsitatea, Faculty of Engineering, Loramendi 4, Arrasate-Mondragón, 20500, Spain

* Corresponding author. Tel: +(34) 943794700. *E-mail address:* amadariaga@mondragon.edu

Abstract

Aerostructures withstand cyclic mechanical loads and therefore, their design must fulfil surface integrity and fatigue strength requirements. This paper studies the effect of pneumatic machine hammer peening on surface integrity of 7050-T7451 aluminium alloy. Specimens were hammer peened using two different stepover distances (0.07 and 0.35 mm) and initial offset (0.3 and 0.5 mm). A Kistler dynamometer was used to measure the forces generated by hammer peening. Then, the surface topography, residual stresses and microstructural damage of the specimens were characterised. The results demonstrate that the magnitude of residual stresses and the thickness of the affected layer increases when reducing the stepover distance, while surface roughness reduces. Additionally, none of the tested conditions produced microstructural defects. These findings suggest that pneumatic hammer peening is an additional process to manufacture thin-walled structural aluminium alloy components.

Keywords: aluminium alloy, hammer peening, residual stresses, roughness

1. Introduction

There is an increasing demand for manufacturing lightweight aircrafts that will enable the reduction of CO_2 and NOx emissions. This has promoted the manufacturing of large aluminium thin-walled monolithic parts in the main structure and load bearing components of the aerospace industry, due to their high specific strength and good forming properties [1]. Furthermore, the durability of the airframe must be carefully considered in the design of aeroplanes [2], and particularly the fatigue and corrosion performance of thin-walled aluminium parts [3]. The in-service fatigue and corrosion behaviour of these parts is strongly linked to the Surface Integrity (SI) of the manufactured component. Beyond this context, the guarantee of SI becomes primary objective for researchers to accomplish [4], to prevent from early in-service failures or avoid surface re-works.

Thin-walled aluminium structural parts are produced by high-speed machining, removing a high amount of material (up to 90%) from the original workpiece [5], and thus finishing machining operations affect the final SI. For this reason, some researchers have analysed the effect of machining parameters on the SI of aluminium alloys [3-4, 6-11]. Ammula and Guo [6] found that cutting speed had a dominant effect on average surface roughness, but Perez et al. [3] did not measure significant variations in roughness values when milling 7050-T7451 aluminium alloy at several cutting speed. Generally, most authors have found more compressive residual stresses in aluminium alloys employed in the aerospace industry when increasing the cutting speed [3, 8, 10, 11] and increasing the

10.1016/j.procir.2022.03.053

feed-rate [8,9].

These advances enable manufacturers to machine parts with enhanced SI and in-service performance. To further improve the SI of thin-walled aluminium parts, shot-peening is frequently applied after machining. During shot-peening hard balls with high kinetic energy impact the surface, inducing beneficial compressive residual stresses and work hardening. Some authors have analysed the effect of shot-peening on the SI of aluminium alloys used in aircraft structural components [12-15]. Zupan and Grum [12] found that higher shot-peening intensities generated slightly rougher surfaces but also higher microhardness and compressive residual stresses (Ra =5.81 µm, 220 $HV_{0.3}$, -325 MPa) than low intensities (Ra = 4.57 µm, 205 $HV_{0.3}$, -300 MPa) in 7075-T651 alloy. Both intensities affected a layer with a thickness of ≈ 400 µm. Yao et al. [13] also observed compressive residual stresses (≈ -240 MPa) when shot-peening the 7055-T77 aluminium alloy, but they found a reduction of hardness compared to the raw material. More recently, Zagar et al. [14] analysed the effect of shot-peening on SI of specimens of aluminium alloy 7050 with different heat-treatments. They reported maximum compressive residual stresses ranging from -150 to -250 MPa, being the most compressive when shot-peening the age hardened specimens. Interestingly, Pandey et al. [15] demonstrated that ultrasonic shot-peening (USSP) successfully induces a nanostructure layer in the surface region of the peak aged 7075 aluminium alloy.

Machine hammer peening (MHP) with guided tools is a relatively new mechanical surface treatment and it is gaining more importance in industrial applications for improving fatigue behaviour or corrosion performance of structural components [16]. During continuous contact machine hammer peening process, the tool is initially moved down to ensure the contact with the part, and then, the head of tool advances in the main direction and impacts the surface of the part with a hammering frequency. This process generates compressive residual stresses and a strain-hardened layer due to the plastic deformation. Furthermore, some authors have observed microstructural changes, basically generation of ultra-fine grains which contributes to the fatigue life improvement [17]. One of the advantages of MHP is that it can be applied in the same machine that is used for the machining process, whilst shot-peening requires moving the part to another equipment. MHP process has been applied to a variety of materials as summarised in the review of Schulze et al. [16], but there is a lack of research in aluminium alloys. Lin et al. [18] studied the surface modification of 6016 anodized aluminium alloy using piezoelectric machine hammer peening. They found that increasing hammering frequency produces smoother surfaces and higher hardness. An interesting alternative to piezoelectric machine hammer peening is the pneumatic machine hammer peening, since machine tool investment is much lower. In a recent study, Sarasua et al. [19] obtained compressive residual stresses up to 600 µm depth when using this technique to treat the nickel-based alloy Inconel 718. Therefore, it seems to be a suitable approach to obtain thick compressed layers in ductile materials, such as aluminium alloys.

This work aims to understand the effect of pneumatic machine hammer peening on surface integrity of 7050-T7451 aluminium alloy. For that purpose, machine hammer peening tests were carried out, machining forces were measured during the tests and the surface integrity (microstructural alterations, surface roughness and residual stresses) of the hammer peened specimens were characterised. Complementarily, the productivity of the machine hammer peening process is also addressed.

2. Materials and experiments

2.1. Manufacturing of specimens

The aluminium alloy 7050-T7451 widely used in the manufacturing of aerostructural components was selected for this work. A 200 mm long, 50 mm wide and 10 mm thick specimen was extracted by water jet assisted machining from a 40 mm thick plate. The longest side of the specimen was aligned with the rolling direction of the original aluminium plate. The selected material had a yield stress of 470 MPa, a rupture stress of 574 MPa and a Young's modulus of 71 GPa. Before the hammer peening tests, the upper and lower surfaces of the specimen were face milled in the CNC Kondia B1050 machine using an indexable face milling cutter and uncoated inserts. Smooth milling conditions were used to avoid the generation of significant machining-induced residual stresses. The hammer peening tests were done in the same CNC Kondia B1050 machine. For that purpose a FORGEfix pneumatic hammer peening tool was fixed in the tool holder of the CNC machine. The specimen was fixed to a triaxial sensor Kistler dynamometer (9272) in order to measure the forces generated by the hammer peening tests in three orthogonal directions. This set-up is shown in Fig. 1.

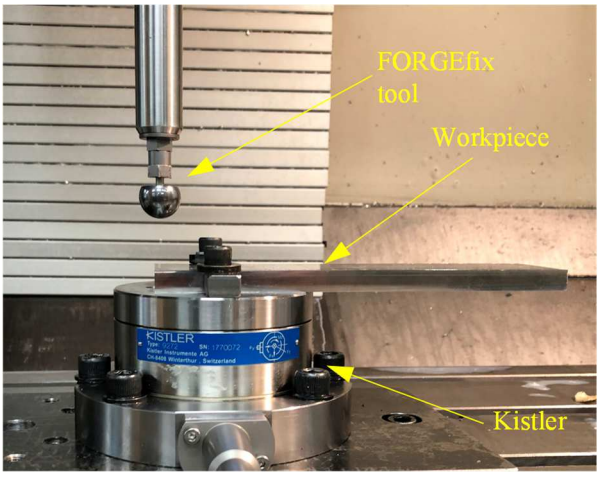

Fig. 1. Set-up used in the hammer peening tests.

A total of four different hammer peening conditions were tested as shown in Fig. 2. The hammer peening process was applied as follows: i) the tool was moved down an initial offset (Z_0), ii) then the tool advanced in the X direction from the left to the right at feed v, iii) when reaching the end of the trajectory, the tool was raised and moved back to the left position and iv) finally, the tool was laterally displaced by the stepover

distance (s). The previous steps were repeated to treat the target area. It should be clarified that the worpiece was positioned in each step to ensure that the target area was centered in the Kistler dynamometer. Table 2 summarises the parameters used in the hammer peening tests. The stepover distance and initial offset were modified in the tests. The range of values for the stepover distance were decided based on tool manufacturer recommendations. The initial offset Z_0 is the thickness of material that we initially compress, but some elastic recovery can occur. Some preliminary tests were carried out varying Z_o from 0.1 to 1 mm. We tried Z_0 = 1 mm to induce higher plastic deformation but the tool broke. Thus, for the final tests the value of Z_o was limited from 0.3 mm to 0.5 mm; to ensure contact between the tool and the surface, but avoid any risk of tool failure. However, the feed, hammering frequency ($f \approx 250$ Hz) and the diameter of the cemented carbide indenter (d = 20 mm) and the air supply ($\approx$ 6 bar) were not changed.

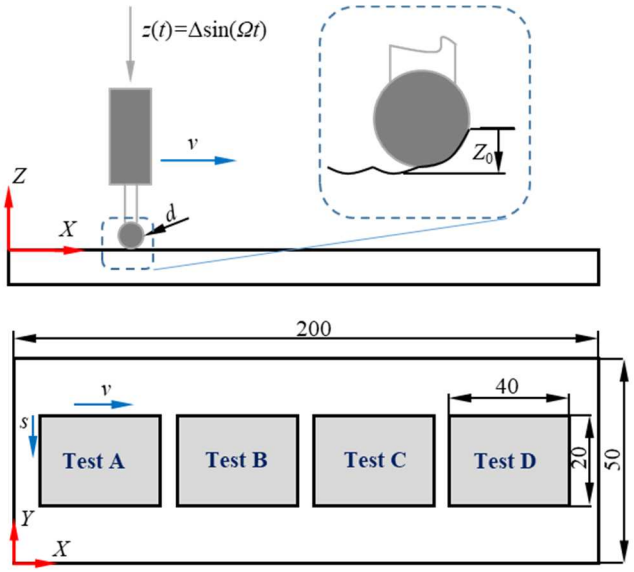

Fig. 2. Scheme of the hammer peening tests.

Table 1. Parameters used in hammer peening tests.

Test	v (m·min^{-1})	s (mm)	Z_0 (mm)	d (mm)	f (Hz)
A	5	0.35	0.3	20	≈250
B	5	0.07	0.3	20	≈250
C	5	0.35	0.5	20	≈250
D	5	0.07	0.5	20	≈250

2.2. Surface Integrity characterisation

The roughness of the machined surface and four hammer peened surfaces was measured in both the feed direction (X) and the stepover direction (Y) employing a contact roughness tester Mitutoyo SJ-210. The average surface roughness Ra, the total height of the roughness profile Rt and the mean roughness depth Rz of the hammer peened surfaces was measured following the UNE-EN ISO 4288:1998 Standard. The parameters employed in the measurements were: 2 µm stylus tip radius, filtering of the measured profile with a cut-off wavelength λ_s = 2.5 µm and filtering of the primary profile with the cut-off wavelength λ_c = 0.8 mm, and evaluation length of 5 times λ_c.

The residual stresses induced by machining and the hammer peening were measured by the hole drilling technique, following the procedure explained in the ASTM-E357 standard. The strain gauges CEA-062UL-120 supplied by Vishay Measurement Group were bonded in the centre of the hammer peened surfaces to characterise the residual stresses. The surfaces were prepared for gauge installation following the instructions of the gauge supplier. The tests were carried out using a Restan MTS3000 machine equipped with a high speed air turbine. The drill bits had a diameter of 1.6 mm. The drill bit was aligned with the gauge before drilling the hole. The zero depth was detected by electrical contact between the drill bit and the workpiece surface. Then, the incremental hole drilling procedure was carried out at each gauge employing a total of 15 depth increments: five initial increments of 20 µm, the next six increments of 50 µm, and the final four increments of 100 µm. This sequence of increments made a hole with a $\approx$ 1.8 mm diameter and a depth of 800 µm. Strains were recorded in a HBM data acquisition system after each increment. Finally, the residual stress profiles were calculated following the method described in the ASTM-E357.

The samples for microstructural analysis were cut out from the machined surface and four hammer peened surfaces. The microstructure was observed in two directions: in the longitudinal direction (X, parallel to the feed direction) and in the transverse direction (Y, parallel to the stepover direction). These samples were hot mounted in a phenolic resin with carbon filler, ground employing Silicon Carbide papers and polished to obtain the desired surface quality. Then, the samples were chemically etched using Keller's reagent. The microstructure of the samples was observed in a Leica DMi8 optical microscope.

3. Results and discussion

3.1. Forces during hammer peening

The hammer peening forces varied during the process, and reached peak values when impacting the treated surfaces. The average of the peak forces in the feed direction (X), stepover direction (Y) and perpendicular to the surface (Z) are shown in Fig. 3. The higher forces were found in the Z direction, ranging from 660 to 780 N, since these are linked to the contact forces. The maximum forces in the feed direction (X) were much lower than in the Z direction, ranging from 210 to 290 N. The peak forces in the X direction varied from 240 to 290 N. The forces in the X direction are mainly generated by the friction between the tool and workpiece in the main sliding motion. Finally, it should be noted that the forces in the stepover direction (Y) were very low 65 N.

The influence of the initial offset Z_0 on the average of the peak forces was not significant for the tested conditions.

Nevertheless, the maximum forces perpendicular to the surface increased when reducing the stepover distance: 10% when using $Z_0 = 0.3$ mm, and 18% when using $Z_0 = 0.5$ mm. Each impact plastically deforms and hardens the surface layer, and when reducing the stepover distance the tool impacts more times on the hardened surface. Consequently, the contact forces increase when employing lower stepover values. The influence of the stepover distance on the forces in the *X* direction was not evident, since contradictory trends were observed when using $Z_0 = 0.3$ mm and $Z_0 = 0.5$ mm. Finally, the variation of the forces in the *Y* direction was not significant, because these changes were within the uncertainty range.

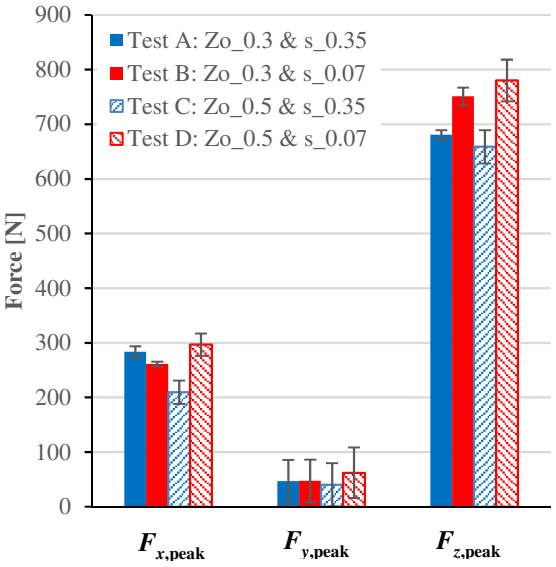

Fig. 3. Average of maximum forces during hammer peening tests.

3.2. Roughness

Fig. 4 shows the roughness parameters *Ra*, *Rt* and *Rz* of the hammer peened surfaces in both the longitudinal direction (*X*, feed) and transverse direction (*Y*, stepover direction). The roughness of the machined surface was also measured as reference in both directions. The workpiece was machined using finishing conditions and this produced a smooth surface: *Ra* of 0.16 µm in the longitudinal direction and 0.10 µm in the transverse direction. As it can be seen in Fig. 4, the hammer peening slightly increased these values as consequence of the induced plastic deformation, but *Ra* was below 0.3 µm in all cases. However, this increase in roughness is much lower than the one generated by shot-peening in aluminium alloys. For instance, Yao et al. [14] reported *Ra* > 2.5 µm when applying shot-peening to a milled surface 7055-T77 aluminium alloy, and Zupan and Grum [12] found *Ra* > 4.5 µm in 7075-T651 alloy.

In the longitudinal direction the smoothest surface was obtained when applying the lowest offset Z_0 and stepover distance *s*. In general, roughness parameters *Ra*, *Rt* and *Rz* increased when increasing the initial offset from 0.3 to 0.5 mm. When increasing the initial offset, the maximum contact force F_z increases (see Fig. 3). Some authors have found that roughness ecreases when increasing the contact force up to an optimum value, but roughness increases for further increased contact force [16]. The effect of stepover distance is more evident in the transversal direction; *Ra*, *Rt* and *Rz* decreased by 40-50% when reducing *s* from 0.35 to 0.07 mm. The coverage is increased when reducing the stepover since the same region is subjected to more impacts. Generally, the increase of coverage generates smoother surface [16].

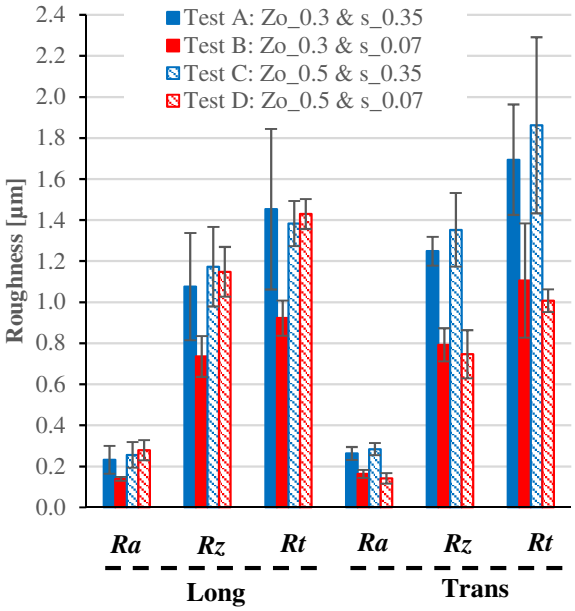

Fig. 4. Roughness of the tested surfaces in both longitudinal (*X*) and transverse direction (*Y*).

3.3. Residual Stresses

Fig 5 shows the initial residual stresses induced by machining and the residual stresses generated by the four hammer peening tests. All the hammer peening test generated compressive residual stresses in both the longitudinal direction (feed motion) and the transverse direction (stepover motion) and they reached a depth higher than 800 µm. The compressive residual stresses were lower in the feed direction than in the in the stepover direction, as observed by other authors [16]. This compressive layer is basically caused by highly localised contact forces. The magnitude of machining-induced residual stresses (from -80 MPa to 50 MPa) and the thickness of the affected layer (< 20 µm) was very low compared to those induced by hammer peening. In fact, the layer affected by residual stresses rarely exceeds 200 µm in depth when applying finishing conditions in aluminium alloys [3, 8, 14]. Furthermore, it is also two times greater than the thickness of the layer affected by high intensity shot-peening [12]. Undoubtedly, these findings suggest that it is possible to improve the fatigue strength or corrosion behaviour of structural aluminium alloy components by hammer peening.

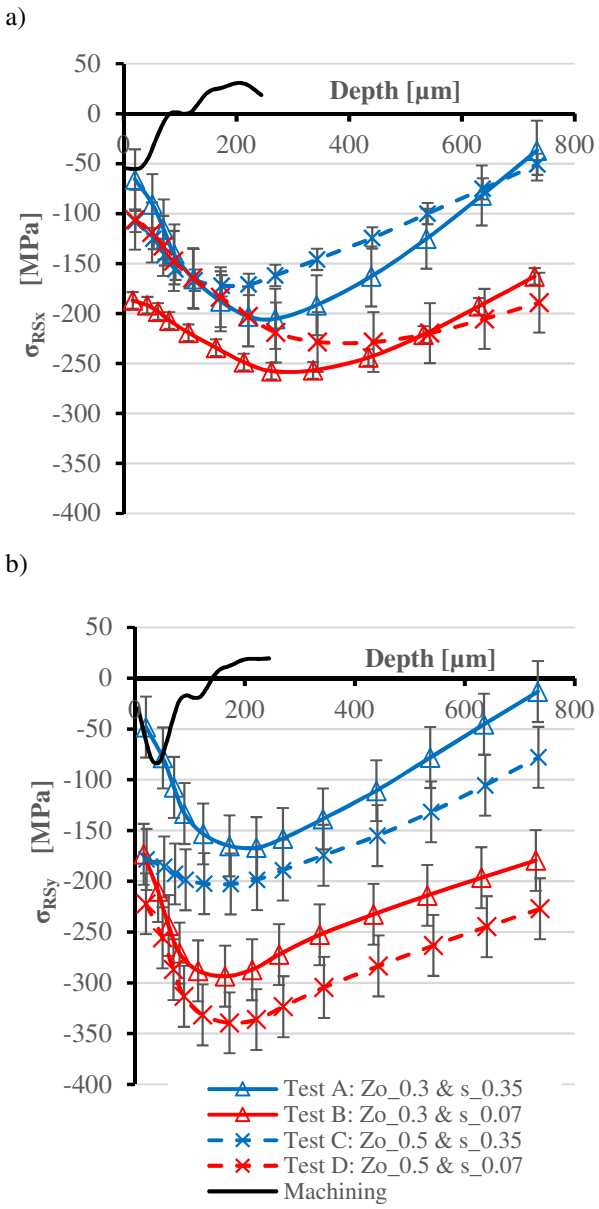

Fig. 5. Residual stress profile in a) the longitudinal direction and b) transverse direction.

Compressive residual stresses were the lowest near the surface, ranging from -60 to -190 MPa in the longitudinal direction and from -50 to -220 MPa in the transverse direction. The maximum compressive residual stress peak was located at a depth of ≈ 250 to 350 µm in the longitudinal direction. The maximum compressive residual stress increased 50-100 MPa when reducing the stepover distance.

The maximum compressive peak was even more compressive in the transverse direction and its value increased up to -300 MPa (≈ 60% of the yield stress of the raw material) when employing the lowest stepover distance. Nevertheless, the position of the maximum compressive peak was closer to the surface than in the longitudinal direction. It should be highlighted that the magnitude of residual stresses at 800 µm depth ranges from -150 to -230 MPa when using the lowest stepover distance. Other authors also reported higher near surface residual stresses when increasing the coverage with pneumatic hammer peening process [20]. However, the effect of the initial offset on the residual stresses is not significant, since no clear trends are observed and changes lay within the uncertainty of the measurements. Therefore, there is a correlation between the forces induced by hammer peening in the *Z* direction and the magnitude of residual stresses and affected layer, since these forces increased when reducing the stepover distance but did not vary when changing the initial offset value.

3.4. Microstructural alterations

Fig. 6 shows the microstructure of the machined surface, and Fig.7 and 8 show examples of the microstructure of the hammer peened surface in the feed direction (*X*) and stepover direction (*Y*). The microstructural observations did not reveal significant defects either in the machined surface or hammer peened surface. There were only identified slightly bent grains below 3 µm depth in localised regions. None of the analysed conditions resulted in major defects. Based on the criteria of the aeronautical industry, it can be concluded that the surface layer affected by the hammer peening conditions is acceptable (lower than 3 µm) and the four conditions analysed in this paper could be used in industry applications.

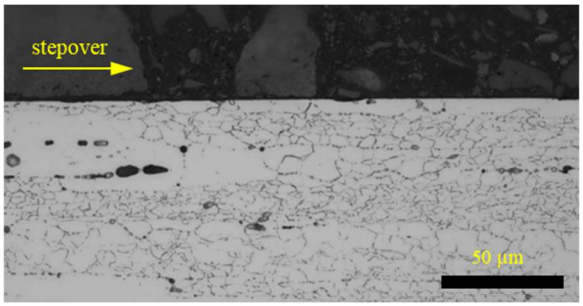

Fig. 6. Microstructure of the machined surface in the stepover direction.

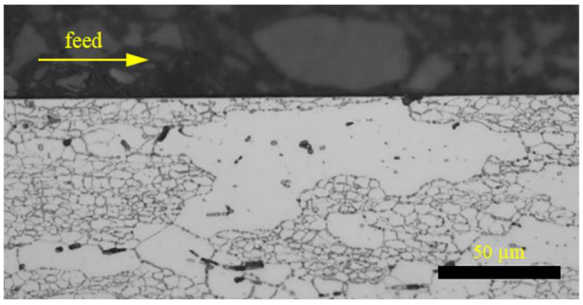

Fig. 7. Microstructure of the surface D in the feed direction.

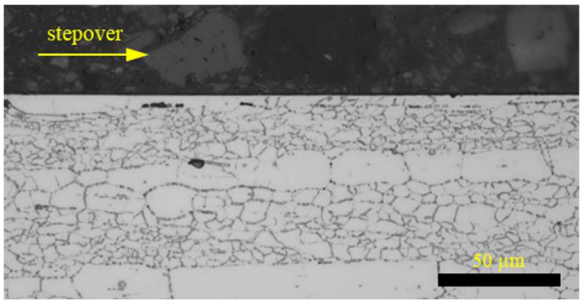

Fig. 8. Microstructure of the surface B in the stepover direction.

3.5. Productivity

The previous sections demonstrate that pneumatic hammer peening can generate components with enhanced surface integrity. Nevertheless, the productivity of this process should be discussed before transferring to industry. In this study, the lowest stepover distance required 1.75 s to treat 1 mm^2, and 0.35 s when using the highest stepover distance. A long period would be required to apply hammer peening to the entire surface of a large thin-walled aluminium structural component. However, manufacturing costs can be significantly reduced if only the critical surfaces are hammer peened.

4. Conclusions

This study was focused on the analysis of SI produced by pneumatic hammer peening in A7050-T7451 aluminum alloy. The main conclusions of this work are the following:

- The contact forces generated during hammer peening increase when reducing the stepover distance. However, forces in the feed and stepover motion direction do not vary significantly for the tested range of conditions.
- None of the analysed hammer peening parameters caused major defects. There were only identified bent grains below 3 µm depth in localised regions.
- The roughness slightly increased with respect to the machined surface when applying hammer peening, but it still showed low values (Ra < 0.3 µm). The reduction of stepover also resulted in reduction of roughness, mainly in the stepover motion direction.
- All tested conditions generated compressive residual stresses, being more compressive in the stepover direction. The magnitude and thickness of the compressive layer increased significantly when reducing the stepover distance.
- Based on the results of this study, pneumatic hammer peening is an alternative to shot-peening to manufacture components with enhanced surface integrity.

This work has demonstrated the capability of pneumatic machine hammer peening to produce aluminum alloy parts with enhanced surface integrity. Nevertheless, future work is necessary to further optimise the process conditions. Experimental work combined with numerical methods should study the effect of indenter diameter, feed and pressure on SI.

Acknowledgements

This work was funded by the “Desarrollo Económico e Infraestructuras” department of the Basque Government (ELKARTEK program, project PROCODA KK-2019/00004).

References

[1] Fridlyander IN. Aluminum Alloys in Aircraft in the Periods of 1970–2000 and 2001–2015. Metal Sci Heat Treat 2001: 43(1):6-10.

[2] Campbell FC. Manufacturing technology for aerospace structural materials. 1st ed. Elsevier; 2006.

[3] Perez I, Madariaga A, Cuesta M, Garay A, Arrazola PJ, Ruiz JJ, Rubio FJ, Sanchez R. Effect of cutting speed on the surface integrity of face milled 7050-T7451 aluminium workpieces.Procedia Cirp 71 2018: 460-465.

[4] Yao CF, Dou X, Wu D, Zhou Z, Zhang J. Surface integrity and fatigue analysis of shot-peening for 7055 aluminum alloy under different high-speed milling conditions. Adv Mech Eng 2016; 8(10):1687814016674628.

[5]Li JG, Wang SQ. Distortion caused by residual stresses in machining aeronautical aluminum alloy parts: recent advances. Int J Adv Manuf Technol 2017; 89(1):997-1012.

[6] Ammula SC, Guo YB. Surface integrity of Al 7050-T7451 and Al 6061-T651 induced by high speed milling. SAE Technical Paper, 2005.

[7] Zhong Z, Ai X, Liu Z, Liu J, Xu Q. Surface morphology and microcrack formation for 7050-T7451 aluminum alloy in high speed milling. Int J. Adv Manuf Technol 2015; 78(1):281-296.

[8] Denkena B, Boehnke D, De Leon L. Machining induced residual stress in structural aluminum parts. Prod Engineer 2008; 2(3):247-253.

[9] Masoudi S, Amini S, Saeidi E, Eslami-Chalander H. Effect of machining-induced residual stress on the distortion of thin-walled parts. Int J Adv Manuf Technol 2015; 76(1-4):597-608.

[10] Huang X, Sun J, Li J, Han X, Xiong Q. An experimental investigation of residual stresses in high-speed end milling 7050-T7451 aluminum alloy. Adv Mech Eng 2013: 5:592659.

[11] Jeelani S, Biswas S, Natarajan R. Effect of cutting speed and tool rake angle on residual stress distribution in machining 2024-T351 aluminium alloy—unlubricated conditions. J Mater Sci 1986; 21(8):2705-2710.

[12] Žagar S, Markoli B, Naglič I, Šturm R. The Influence of Age Hardening and Shot Peening on the Surface Properties of 7075 Aluminium Alloy. Mater 2021; 14(9): 2220.

[13] Zupanc U, Grum J. Surface integrity of shot peened aluminium alloy 7075-T651. Strojniški vestnik-J Mech Eng 2011; 57(5): 379-384.

[14] Yao C, Ma L, Du Y, Ren J, Zhang D. Surface integrity and fatigue behavior in shot-peening for high-speed milled 7055 aluminum alloy. Proc Inst Mech Eng Part B: J Eng Manuf 2017; 231(2): 243-256.

[15] Pandey V, Singh JK, Chattopadhyay K, Srinivas NS, Singh V. Influence of ultrasonic shot peening on corrosion behavior of 7075 aluminum alloy. J Alloy Compd 2017; 723: 826-840.

[16] Schulze V, Bleicher F, Groche P, Guo YB, Pyun YS. Surface modification by machine hammer peening and burnishing. Cirp Annals 2016; 65(2): 809-832.

[17] Chan WL, Cheng HKF. Hammer peening technology—the past, present, and future. The International Journal of Advanced Manufacturing Technology 2022; 118:683–701

[18] Lin XH, Huang HB, Zhou CS, Liu JC, Saleh M, Wang ZZ. Research on surface modification of anodized aluminum alloy using piezoelectric machine hammer peening. The International Journal of Advanced Manufacturing Technology 2019; 104(1): 1211-1219.

[19] Miranda JAS, Cristobal AT, González-Barrio H, Fernández-Lucio P, Gómez-Escudero G, Madariaga A, Arrazola PJ. Comparative study of finishing techniques for age-hardened Inconel 718 alloy. Journal of Materials Research and Technology 2021; 15: 5623-5634

[20] Hacini L, Leˆ N, Bocher P. Evaluation of Residual Stresses Induced by Robotized Hammer Peening by the Contour Method. Experimental Mechanics 2009; 49: 775–783.